2017

Post-polymerization functionalization of poly(ethylene oxide)–poly(β-6-heptenolactone) diblock copolymers to tune properties and self-assembly

Brooke M. Raycraft

Jarret P. MacDonald

James T. McIntosh

Michael P. Shaver

Post-polymerization functionalization of poly(ethylene oxide)–poly(-6-heptenolactone) diblock copolymers to tune properties and self-assembly

Journal Name

ARTICLE

Post-polymerization functionalization of poly(ethylene oxide)-poly(β-6-heptenolactone) diblock copolymers to tune properties and self-assembly

Received 00th January 20xx,
Accepted 00th January 20xx

DOI: 10.1039/x0xx00000x

www.rsc.org/

Brooke M. Raycraft,[a] Jarret P. MacDonald,[a,b] James T. McIntosh,[a] Michael P. Shaver,[b] and Elizabeth R. Gillies[a,c*]

Polyester-based amphiphilic block copolymers and their nanoassemblies are of significant interest for a wide range of applications due to the degradability of the polyester block. However, the commonly used polyesters lack functional groups on their backbones, limiting the possibilities to chemically modify these polymers. Described here are new poly(ethylene oxide)(PEO)-poly(β-6-heptenolactone) (PHEL) block copolymers having pendant alkenes at each repeat unit on the PHEL block. First, the self-assembly of these block copolymers in aqueous solution was studied and it was found that they formed solid nanoparticles and vesicles depending on the relative block lengths. Next the alkene moieties of the block copolymer were modified with either hydrophilic or hydrophobic pendant groups using thiol-ene reactions, allowing the hydrophilic mass fractions and consequently the self-assembled morphologies to be tuned, accessing both smaller nanoparticles and cylindrical assemblies. It was also demonstrated that the anti-cancer drug paclitaxel or a fluorescent rhodamine dye could be easily conjugated to the block copolymers and the self-assembly of these conjugates was explored. Overall, the results of this study demonstrate that PEO-PHEL block copolymers can serve as versatile backbones for the preparation of functional, polyester-based materials.

Introduction

The self-assembly of block copolymers has attracted considerable attention recently as it can enable the preparation of a wide range of ordered structures including spherical micelles, cylindrical micelles, vesicles, and other morphologies from relatively simple polymeric components.[1-3] It is well established that the morphology can be tuned by varying the polymer composition, molar mass, and the mass or volume fraction of each block (*f*). Polymer assemblies show promise for a number of applications including nanopatterning,[4, 5] nanoelectronics,[6] diagnostics,[7, 8] and drug delivery.[9, 10] They have garnered particular interest as drug delivery vehicles and contrast agents as their nanoscale size is ideal for achieving long *in vivo* circulation times and passive targeting of tumors through the enhanced permeation and retention effect.[11, 12] Drug molecules and contrast agents can be loaded into the hydrophobic or hydrophilic cores of micelles or vesicles respectively while specific targeting moieties can be conjugated to the surfaces of the assemblies.[13]

Of the numerous block copolymer assemblies that have been investigated for biomedical applications, many contain polyesters.[14-20] Polyesters such as poly(lactic acid) (PLA), poly(lactic-co-glycolic acid) (PLGA) and polycaprolactone (PCL) are attractive as they can be broken down through enzymatic or non-enzymatic hydrolysis and have also been demonstrated to be biocompatible in certain applications.[21, 22] For example, a poly(ethylene oxide) (PEO)-PLA micelle containing paclitaxel (PTX) has been approved for treatment of breast, lung, and ovarian cancer in Korea,[23] while a PEO-PLGA micelle containing docetaxel and targeted to prostate-specific membrane antigen is in clinical trials.[24] However, a limitation of the commonly used polyesters is a lack of available pendant groups, making it challenging to tune their physical properties and to conjugate drugs, contrast agents or probes.

Motivated by the interest in polyesters as biomedical materials, but also as degradable and potentially bio-sourced alternatives to conventional non-degradable polymers, there has been significant interest in the development of polyesters with pendant functional groups over the past several years. For example, polyesters with alkenes,[25-32] alkynes,[33, 34] α,β-unsaturated carbonyls,[35, 36] hydroxyls,[33, 37] epoxides,[33] amines,[38] and other functional groups have been prepared through ring-opening and condensation approaches using a wide variety of different monomers. These pendant groups have enabled the tuning of the thermal properties.[28, 30, 33, 37]

[a] *Department of Chemistry and Center for Advanced Materials and Biomaterials Research (CAMBR), The University of Western Ontario, 1151 Richmond St., London, Canada N6A 5B7. Email: egillie@uwo.ca*
[b] *School of Chemistry, University of Edinburgh, Joseph Black Building, David Brewster Road, Edinburgh, EH9 3FJ*
[c] *Department of Chemical and Biochemical Engineering, The University of Western Ontario, 1151 Richmond St., London, Canada N6A 5B9*
Electronic Supplementary Information (ESI) available: Additional experimental procedures, NMR and IR spectra, SEC traces, thermal data, DLS data, CAC measurements, additional TEM. See DOI: 10.1039/x0xx00000x

They have also been derivatized to introduce carboxylic acids,[26] azides,[39], epoxides,[32, 40] amines,[32] sugars,[41] dienes,[29] boronates,[42] and fluoroalkyl chains[34] as well as to perform cross-linking.[31, 40]

Despite the large number of functional polyesters now available, there are only a limited number of block copolymer-based polyesters bearing reactive groups. For example, PEO monomethyl ether was used as an initiator for a ring-opening polymerization of α-benzyl carboxylate-ε-caprolactone (BCL) and for the copolymerization of caprolactone and BCL to afford PEO-*b*-PBCL and PEO-*b*-P(BCL/CL).[43] The sizes and stabilities of micelles prepared from these copolymers depended on the BCL content. The benzyl group could also be cleaved by hydrogenolysis to afford pendant carboxylic acids that were used to conjugate cholesterol[44] or palmitoyl[45] groups in order to enhance the drug compatibility of the micelle core, or PTX to enhance its loading and control its release.[46] In other work, a methanolysis procedure could be applied to poly(3-hydroxyoctanoate-*co*-3-hydroxyundecenoate) to afford low molar mass initiators for the polymerization of caprolactone. Subsequent oxidation of the pendant alkenes to carboxylic acids afforded amphiphilic block copolymers.[47] Alkyne-functionalized *o*-carboxyanhydrides derived from tyrosine have also been prepared and ring opening polymerization from PEO or PLA led to amphiphilic block copolymers that could be functionalized to prepare light-responsive[48] or cancer-targeted micelles.[49]

We describe here a new functional polyester block copolymer platform based on PEO and poly(β-6-heptenolactone) (PHEL). PEO is a water-soluble block with favorable biological properties,[50, 51] while PHEL provides pendant alkene groups for post-polymerization modification.[25, 27, 42] A small library of PEO-*b*-PHEL copolymers was prepared and then thiol-ene chemistry was used to functionalize the alkenes with hydrophilic and hydrophobic groups including octyl, triethylene glycol (TEG) and carboxylic acids, allowing their *f* values to be tuned. The physical properties and self-assembly of the starting polymers and their derivatives were studied and compared. In addition, it was shown that the pendant groups could be used to conjugate PTX and the fluorescent dye rhodamine B, further demonstrating the functionality and versatility of this chemistry.

Results and discussion

Synthesis and characterization of PEO-PHEL block copolymers

β-6-heptenolactone (β-6-HEL) was selected as the monomer for the preparation of functionalizable block copolyesters as it has a pendant terminal alkene that should allow for reactions with thiols *via* thiol-ene chemistry.[52, 53] Previously, β-6-HEL has been polymerized using zinc and yttrium complexes and the resulting polymers were functionalized to introduce hydroxyl, epoxide, and pinacolborane moieties.[25, 42] Recently, Shaver and coworkers demonstrated that that β-lactones undergo controlled coordination insertion ring opening polymerization (ROP) using aluminum salen catalysts.[54] Successful ROP of β-6-HEL was achieved and this was expanded to include the random copolymerization with lactide, followed by cross-metathesis to include a range of functional groups.[27] To the best of our knowledge, β-6-HEL has not previously been incorporated into block copolymers. This monomer was synthesized using a procedure previously reported for similar lactones involving epoxide carbonylation using a chromium porphyrin complex[54] and its identity was confirmed by comparison with previously reported data for the same compound.[55] For the preparation of block copolymers, PEO monomethyl ether with a molar mass of 2000 g mol^{-1} was used as an initiator and the polymerization was conducted in toluene at 85 °C for 20 h using an aluminum salen catalyst[56] (Scheme 1). To prepare block copolymers with varying block ratios, 26, 50, and 90 equivalents of β-6-HEL were used (Table 1). Evaluation of the ^{1}H NMR spectra prior to purification showed that the conversion of β-6-HEL varied from 86-88%. The polymers were subsequently purified by precipitation into hexanes.

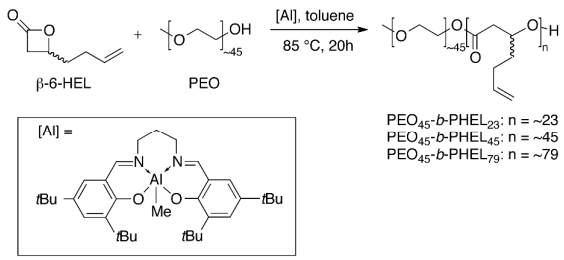

Scheme 1. Synthesis of PEO-*b*-PHEL block copolymers.

Table 1. Composition and properties of the PEO-*b*-PHEL block copolymers.

Copolymer	Equiv. of β-6-HEL added	DP of PHEL (NMR)	M_n (g mol^{-1}) (NMR)	M_n (g mol^{-1}) (SEC)	*Đ* (SEC)	T_g (°C)	T_m (°C)
PEO_{45}-*b*-$PHEL_{23}$	26	23	4576	5140	1.08	-54	35
PEO_{45}-*b*-$PHEL_{45}$	51	45	7040	6630	1.19	-59	29
PEO_{45}-*b*-$PHEL_{79}$	92	79	10848	12910	1.03	-46	22, 29

The block copolymers were characterized by ^{1}H NMR spectroscopy, FTIR spectroscopy, size exclusion chromatography (SEC), thermogravimetric analysis (TGA) and differential scanning calorimetry (DSC) (data included in the ESI). The degree of polymerization (DP) of the polyester block was determined using ^{1}H NMR spectroscopy by comparing the integration of the peak at 3.6 ppm corresponding to the hydrogens on the PEO block with those of the multiplets corresponding to the alkene protons as well as the methine hydrogen on the PHEL block from 5 – 5.8 ppm (Fig. 1 and S1-S3). The results indicated that DPs of approximately 23, 45, and 79 were obtained for copolymers

Journal Name

ARTICLE

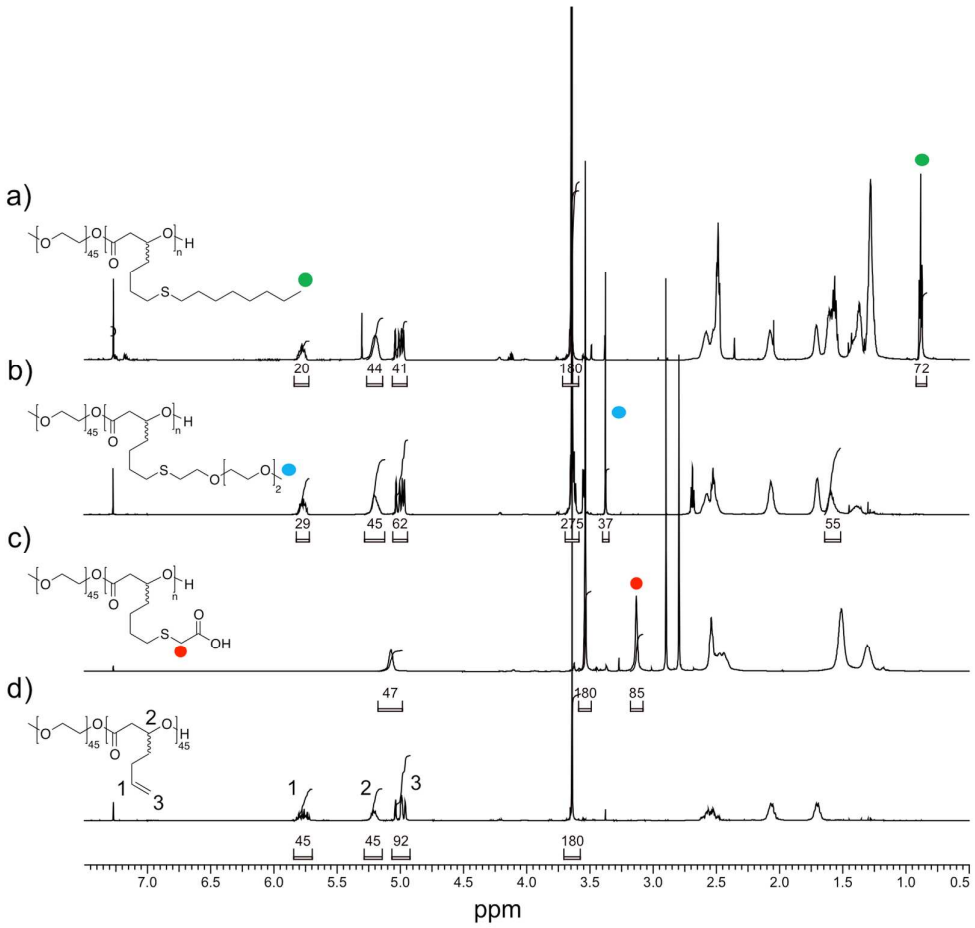

Fig. 1. ^{1}H NMR spectra (600 MHz, $CDCl_3$) of a) PEO_{45}-*b*-$PHEL_{21}$-octyl$_{24}$, b) PEO_{45}-*b*-$PHEL_{31}$-TEG_{14} c) PEO_{45}-*b*-CA_{45} d) PEO_{45}-*b*-$PHEL_{45}$. In the spectrum of PEO_{45}-*b*-$PHEL_{45}$, the DP was calculated from the relative integrations of the peak at 3.6 corresponding to PEO and the peaks from 5 – 5.8 ppm corresponding to the alkene protons labeled 1 and 3 and to the proton labeled 2 on the PHEL backbone (average of these three different ratios). For the functionalized derivatives, conversion was calculated based on the reductions in integrations of the alkene peaks 1 and 3 as well as the integrations of the new peaks corresponding to the characteristic functional groups indicated.

PEO_{45}-*b*-$PHEL_{23}$, PEO_{45}-*b*-$PHEL_{45}$, and PEO_{45}-*b*-$PHEL_{79}$ respectively. From these DPs, the number average molar mass (M_n) was calculated for each polymer (Table 1). These ranged from 4576 g mol^{-1} for PEO_{45}-*b*-$PHEL_{23}$ to 10848 g mol^{-1} for PEO_{45}-*b*-$PHEL_{79}$. The molar masses were also measured by SEC in THF relative to polystyrene standards (Fig. S24). As shown in Table 1, the M_ns were in good agreement with those from NMR spectroscopy and the dispersity (*Đ*) was less than 1.2 for each copolymer. FTIR spectra showed characteristic peaks corresponding to the C=O stretch of the carbonyl and C=C stretch of the alkene on the PHEL block at ~1740 and 1640 cm^{-1} respectively (Fig. S13-S15).

PEO-*b*-PHEL block copolymers were stable up to at least 200 °C as determined by TGA (Table S1). PEO is a highly crystalline polymer with a T_m of ~58 °C[57] while PHEL is an amorphous polymer with a T_g of ~ -40 °C.[25] Upon their incorporation into block copolymers, the resulting materials show both amorphous and crystalline domains, suggesting that they undergo phase separation at the nanoscale (Fig. S26-S28). The T_m of the copolymers decreased from 35 to 22 °C as the PHEL block length increased, suggesting that the crystalline domains became smaller as the PEO content of the copolymers decreased. PEO_{45}-*b*-$PHEL_{79}$ had two melting peaks suggesting the presence of crystalline PEO domains of different sizes. All three of the copolymers underwent cold

crystallization between the T_m and T_g. The T_g ranged from -59 to -46 °C, with no clear trend relating to the changing PHEL block length. However, these T_gs were lower than those previously reported for PHEL of similar DP.[25] Thus, the presence of non-crystalline PEO at these temperatures prior to cold crystallization may enhance segmental motion.

As one of the main goals of this work was to explore the effects of alkene functionalization on the self-assembly of the block copolymers, the self-assembly of PEO_{45}-*b*-$PHEL_{23}$, PEO_{45}-*b*-$PHEL_{45}$, and PEO_{45}-*b*-$PHEL_{79}$ was first explored. The hydrophilic mass fractions (*f*) of the copolymers were calculated as molar mass of PEO block/molar mass of the copolymer and the results are summarized in Table 2. Self-assembly was performed by a solvent exchange process involving first the dissolution of the copolymer in THF, followed by the addition of water and then dialysis to remove the THF. The resulting assemblies were characterized by dynamic light scattering (DLS) (Figs. S36-S38) and TEM to determine their diameters and polydispersity indices (PDI). As shown in Fig. 2a, PEO_{45}-*b*-$PHEL_{23}$ with an *f* of 0.44 assembled into solid spherical nanoparticles and the Z-average diameter measured by DLS was 66 nm, which is in reasonable agreement with the TEM images. This result can be compared with those obtained previously for PEO-*b*-PCL copolymers as the number of carbons in the lactone monomer β-6-HEL is similar to that in caprolactone. Solid spherical nanoparticles were also obtained for similar *f* values in PEO-*b*-PCL copolymers.[58]

Upon decreasing *f* to 0.28 in PEO_{45}-*b*-$PHEL_{45}$, solid spherical nanoparticles with a Z-average diameter of 73 nm were observed (Fig. 2b). This increasing tendency towards the formation of larger assemblies is consistent with the increasing length of the hydrophobic block. In comparison to PEO-*b*-PCL copolymers, typically *f* values between 0.20 and 0.42 result in vesicular morphology. For $f > 0.42$, a mixed morphology of both worm-like micelles and spherical nanoparticles has been observed.[59]

Upon further decreasing *f* to 0.18 in PEO_{45}-*b*-$PHEL_{79}$, vesicles were observed in the TEM images, possibly along with other structures (Fig. 2c). The Z-average diameter of the assemblies measured by DLS increased to 118 nm. As vesicles are more difficult to image by TEM than solid particles due to their tendency to collapse upon drying, they were also imaged by fluorescence confocal microscopy after incorporation of the hydrophobic dye nile red into their membranes. The limitation of this technique is its resolution, which requires the formation of micrometer-sized vesicles. Such vesicles can be obtained by the hydration of polymer films.[60, 61] Thus, PEO_{45}-*b*-$PHEL_{79}$ and 0.1 wt% nile red were dissolved in CH_2Cl_2 and the solution was used to cast a film on a flask. Water was then added, and the suspension was stirred for 24 h. As shown in Fig. 2d, fluorescent vesicles were clearly observed budding from the polymer surface, confirming the tendency of this polymer to form vesicles.

The critical aggregation concentrations (CAC) of all of the above polymer assemblies were measured through encapsulation of the fluorescent probe nile red (Figs. S44-S46).[62] As shown in Table 2, the CAC decreased from 20 to 6 mg L^{-1} with the decreasing *f* values as the length of PHEL block increased. This was expected due to the increased hydrophobicity of the amphiphiles, which would favour self-assembly. However, the differences between these polymers was relatively modest and all CACs were on the same order of magnitude.

Table 2. Hydrophilic mass fraction of polymers and their self-assembly properties as determined by TEM and DLS.

Copolymer	Hydrophilic mass fraction (*f*)	Z-average diameter (nm)	PDI	Morphology	CAC (mg L^{-1})
PEO_{45}-*b*-$PHEL_{23}$	0.44	66 ± 0.5	0.20 ± 0.01	Solid spherical nanoparticles	20
PEO_{45}-*b*-$PHEL_{45}$	0.28	73 ± 1.1	0.34 ± 0.05	Solid spherical nanoparticles	14
PEO_{45}-*b*-$PHEL_{79}$	0.18	118 ± 2.2	0.31 ± 0.01	Vesicles	6

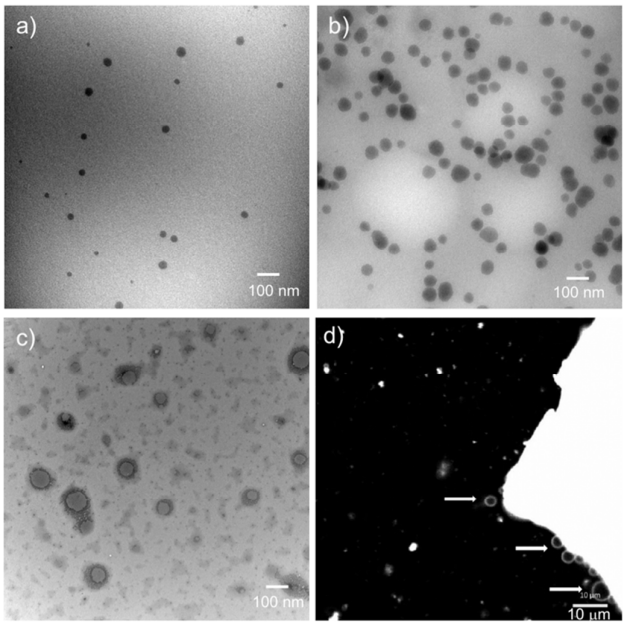

Fig. 2. a-c) TEM images and d) fluorescence confocal microscopy image of assemblies formed from a) PEO_{45}-*b*-$PHEL_{23}$, b) PEO_{45}-*b*-$PHEL_{45}$, and c) PEO_{45}-*b*-$PHEL_{79}$ by the THF/water solvent exchange method and d) PEO_{45}-*b*-$PHEL_{79}$ by film hydration. The arrows in d) show vesicles budding from the surface of solid polymer.

Functionalization of PEO-*b*-PHEL block copolymers to tune hydrophilic fractions and self-assembly

With the block copolymers in hand, the functionalization of the pendant alkenes by thiol-ene chemistry was explored. PEO_{45}-*b*-$PHEL_{45}$ was chosen for this work as it had an intermediate *f* among the three copolymers and it was proposed that it would therefore be possible to modify the polymers to achieve a range of effects on the resulting

assemblies. First, the modification of the copolymer with hydrophobic 1-octanethiol moieties was investigated. PEO_{45}-*b*-$PHEL_{45}$ was reacted with 25 equiv. per polymer chain of 1-octanethiol using 2,2-dimethoxy-2-phenylacetophenone (DMPA) as a photoinitiator in combination with UV irradiation to afford the functionalized copolymer PEO_{45}-*b*-$PHEL_{21}$-$octyl_{24}$ (Scheme 2). The product was purified by dialysis in *N*,*N*-dimethylformamide (DMF). As shown in Fig. 1, the integration of the peak corresponding to the alkene protons at 5.0 ppm in the ^{1}H NMR spectrum decreased from 91 to 41, which is consistent with reacting approximately 24 of the 45 alkenes. In addition, new peaks appeared at 0.88, 1.28, 1.38 and 1.58 ppm that correspond to protons on the alkyl chain. Furthermore, there was a reduction in the C=C stretch peak in the FTIR spectrum (Fig. S16). The M_n of the polymer measured by SEC increased from 6630 to 8150 g/mol, consistent with the increased mass to the polymer. However, it did not increase to the same extent as the actual mass added, which can likely be attributed to the grafted architecture. *Đ* remained unchanged. DSC analysis showed that the T_g and T_m of the polymers were also relatively unchanged in comparison with PEO_{45}-*b*-$PHEL_{45}$ at -60 and 34 °C, respectively (Table 3).

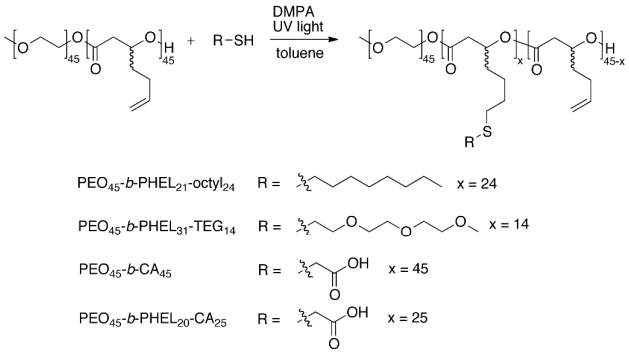

Scheme 2. Functionalization of PEO_{45}-*b*-$PHEL_{45}$ with octyl chains, TEG, and carboxylic acids.

Next, functionalization of PEO_{45}-*b*-$PHEL_{45}$ with 25 equiv. of hydrophilic 1-mercapto-3,6,9,12-tetraoxotridecane (TEG-thiol) moieties was performed using the same conditions described above to afford PEO_{45}-*b*-$PHEL_{31}$-TEG_{14}. As shown in Fig. 1, a reduction in the integration of the alkene peak at 5.0 ppm from 91 to 62 was observed, suggesting that ~14 alkenes were functionalized. In addition, a new peak appeared at 3.36 ppm corresponding to the terminal methoxy group of the TEG chain. A small increase in M_n to 7710 g mol^{-1} relative to the starting PEO_{45}-*b*-$PHEL_{45}$ was measured by SEC while *Đ* remained similar at 1.15. In comparison to PEO_{45}-*b*-$PHEL_{45}$, PEO_{45}-*b*-$PHEL_{31}$-TEG_{14} has a somewhat elevated T_g of -44 °C, suggesting that the TEG grafts reduce segmental motion. However, the T_m remained unchanged.

An additional approach to tune the hydrophilicity and functionality of the block copolymers involved the conjugation of thioglycolic acid to the alkene pendant groups. In this case, either 140 or 27 equiv. per polymer chain were coupled to PEO_{45}-*b*-$PHEL_{45}$ to afford PEO_{45}-*b*-CA_{45} and PEO_{45}-*b*-$PHEL_{40}$-CA_{25} respectively. When 140 equiv. were added, complete functionalization of the alkenes was achieved as shown in Fig. 1 by the disappearance of alkene peaks at 5.0 ppm in the ^{1}H NMR spectrum and the appearance of a peak at 3.1 ppm corresponding to the protons α to the carboxylic acid. When 27 equiv. were used, ~25 carboxylic acid moieties per polymer chain were introduced (Fig. S7). The presence of carboxylic acids on the polymer made it impossible to obtain measurements by SEC due to interactions with the columns. In comparison with PEO_{45}-*b*-$PHEL_{45}$, DSC analysis showed that PEO_{45}-*b*-CA_{45} had a significantly elevated T_g of -19 °C and no T_m. It is possible that hydrogen bonding occurs between the carboxylic acids, reducing segmental motion of the polyester block and preventing the crystallization of the PEO block. For PEO_{45}-*b*-$PHEL_{20}$-CA_{25}, DSC analysis indicated only a slight change in T_g (-46˚C) relative to that of PEO-*b*-$PHEL_{45}$, suggesting that the lower degree of acid functionalization results in less hydrogen bonding. However, there was still no T_m, showing that the acids still inhibited crystallization of PEO.

Table 3. Structures and properties of functionalized PEO_{45}-*b*-$PHEL_{45}$ copolymers. ND = none detected.

Sample	Number of functionalized alkenes	M_n (g mol^{-1}) (NMR)	M_n (g mol^{-1}) (SEC)	*Đ*	T_g (°C)	T_m (°C)
PEO_{45}-*b*-$PHEL_{21}$-$octyl_{24}$	24	10549	8150	1.19	-60	34
PEO_{45}-*b*-$PHEL_{31}$-TEG_{14}	14	9577	7710	1.15	-44	29
PEO_{45}-*b*-CA_{45}	45	11180	-	-	-19	ND
PEO_{45}-*b*-$PHEL_{20}$-*b*-CA_{25}	25	9341	-	-	-46	ND
PEO_{45}-*b*-$PHEL_{11}$-PTX_{34}	34 PTX, 11 acid	39600	9010	1.88	131	ND
PEO_{45}-*b*-$PHEL_{27}$-PTX_{18}	18 PTX, 7 acid	24390	6750	1.30	87	ND
PEO_{45}-*b*-$PHEL_{40}$-RHD_5	5	9895	6300	1.15	-33	ND

As shown in Table 4, following the formula of mass of PEO/total mass of the copolymer, the attachment of 24 octyl chains in PEO_{45}-*b*-$PHEL_{21}$-$octyl_{24}$ results in a decrease in *f* to 0.19 from 0.28 for PEO_{45}-*b*-$PHEL_{45}$. For PEO_{45}-*b*-$PHEL_{31}$-TEG_{14}, *f* was calculated as (mass of PEO + mass of TEG)/total mass of copolymer, resulting in an *f* of 0.47. On the other hand, *f* values were not calculated for the carboxylic acid-functionalized copolymers as it was not obvious what mass should be deemed to contribute to hydrophilicity and the charge of the ionized acids was anticipated to override any calculated changes in *f*.

Self-assembly of the resulting functionalized copolymers was studied in the same manner described above. Upon the addition of octyl chains in PEO_{45}-*b*-$PHEL_{21}$-$octyl_{24}$, "worm-like" assemblies as observed by TEM with lengths on the order of a few hundred nm were formed (Fig. 3a). DLS suggested a Z-average diameter of 143 nm, but the meaning of this number is limited due to the non-spherical nature of the assemblies. It is interesting that although PEO_{45}-*b*-$PHEL_{21}$-$octyl_{24}$ and PEO_{45}-*b*-$PHEL_{79}$ had very similar *f* values, they assembled to different morphologies. This emphasizes that the specific chemical structure and architecture of the amphiphile can have a significant effect on the assembled morphology.

Table 4. Hydrophilic mass fractions of polymers and their self-assembly properties as determined by TEM and DLS.

Copolymer	Hydrophilic mass fraction (*f*)	Z-average diameter (nm)	PDI	Morphology	CAC (mg/L)
PEO_{45}-*b*-$PHEL_{21}$-$octyl_{24}$	0.19	143 ± 4	0.29 ± 0.01	Worm-like assemblies	12
PEO_{45}-*b*-$PHEL_{31}$-TEG_{14}	0.47	59 ± 0.1	0.258 ± 0.002	Solid spherical nanoparticles	41
PEO_{45}-*b*-$PHEL_{20}$-CA_{25}	-	97 ± 3	0.37 ± 0.10	Solid spherical nanoparticles	40
PEO_{45}-*b*-CA_{11}-PTX_{34}	0.05	-	-	Macroscopic aggregation	-
PEO_{45}-*b*-$PHEL_{20}$-CA_7-PTX_{18}	0.08	> 1000	-	Aggregates of nanoparticles	10
PEO_{45}-*b*-$PHEL_{40}$-RHD_5	0.18	102 ± 0.4	0.178 ± 0.007	Solid spherical nanoparticles	16

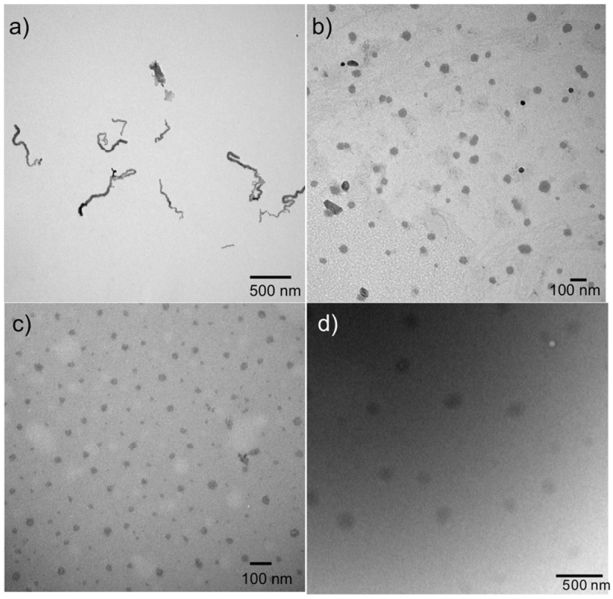

Fig. 3. TEM images of assemblies formed from: a) PEO_{45}-*b*-$PHEL_{21}$-$octyl_{24}$; b) PEO_{45}-*b*-$PHEL_{31}$-TEG_{14}; c) PEO_{45}-*b*-$PHEL_{20}$-CA_{25}; d) PEO_{45}-*b*-$PHEL_{40}$-RHD_5 using the THF/water solvent exchange method.

Alternatively, the attachment of hydrophilic TEG chains in PEO_{45}-*b*-$PHEL_{31}$-TEG_{14} led to nanoparticles with a Z-average diameter of 59 nm (Fig. 3b). By TEM, these assemblies were noticeably smaller than those observed for PEO_{45}-*b*-$PHEL_{45}$ (Fig. 2b). This can be explained by the increased hydrophilicity of the copolymers, which can stabilize smaller nanoparticles. PEO_{45}-*b*-CA_{45} did not yield any well-defined assemblies based on DLS or TEM. However, PEO_{45}-*b*-$PHEL_{20}$-CA_{25} self-assembled to form small nanoparticles (diameter < 40 nm) based on TEM (Fig. 3c). Some aggregation was evident in the DLS, increasing the Z-average size to 97 nm (Table 4, Fig. S41).

The CACs of the copolymers were measured through encapsulation of nile red (Table 4, Fig. S47-S51).[62] While all CACs remained on the same order of magnitude as the initial PEO_{45}-*b*-$PHEL_{45}$, there was a general trend that hydrophobic modifications decreased the CAC and hydrophilic modifications increased it. Thus, while not all modifications led to well-defined assemblies, it was possible to tune the morphologies and stabilities of the polymer assemblies through functionalization of the polyester block. Tuning of morphology through post-polymerization functionalization of block copolymers has also recently been demonstrated using PEO-poly(allyl glycidyl ether) block copolymers,[63] but our system offers the advantage of degradability of the polyester block.

Functionalization of PEO-*b*-PHEL block copolymers with drugs and fluorophores

In addition to altering the hydrophilic-hydrophobic ratios of the polymers, it was also of interest to use the pendant alkene groups to impart other functions. To demonstrate this, PTX and a rhodamine dye (RHD) were conjugated to the copolymers. Copolymer nanoparticles have been widely

investigated as drug delivery vehicles, in particular for anti-cancer treatment due to the possibility of passively and/or actively targeting these systems to tumors.[12, 13] However, a major challenge is poor retention of the drug in the delivery vehicle after its administration. Chemical conjugation of the drug has been shown to eliminate or reduce the burst release effect, enabling slow and prolonged release of drug.[64,65] PTX was selected as the drug to conjugate as it is a widely used anti-cancer therapeutic and is challenging to administer due to its poor water solubility. A number of delivery systems for PTX have been developed and covalent conjugation has been shown to slow and control its release.[46, 66-68]

In designing a chemical conjugation strategy, a mechanism for release of the active drug should be considered. As PTX possesses three hydroxyl groups, with one selectively undergoing esterification,[69, 70] an ester linkage between PTX and PEO_{45}-*b*-$PHEL_{45}$ was targeted. Reaction of PEO_{45}-*b*-CA_{45} with 100 equiv. of PTX per polymer chain using 1-ethyl-3-(3-dimethylaminopropyl) carbodiimide hydrochloride (EDC·HCl) and 4-dimethylaminopyridine (DMAP) afforded PEO_{45}-*b*-CA_{11}-PTX_{34} (Scheme 3). The amount of PTX coupled was determined using ^{1}H NMR spectroscopy by comparing the integration of the peak corresponding to the methine hydrogen on the PHEL block (labeled 1' in Fig. 4) at 5.21 ppm with that of the methine proton adjacent to the amide group on PTX (labeled b' on the chemical structure in Fig. 4) at 5.95 ppm. This

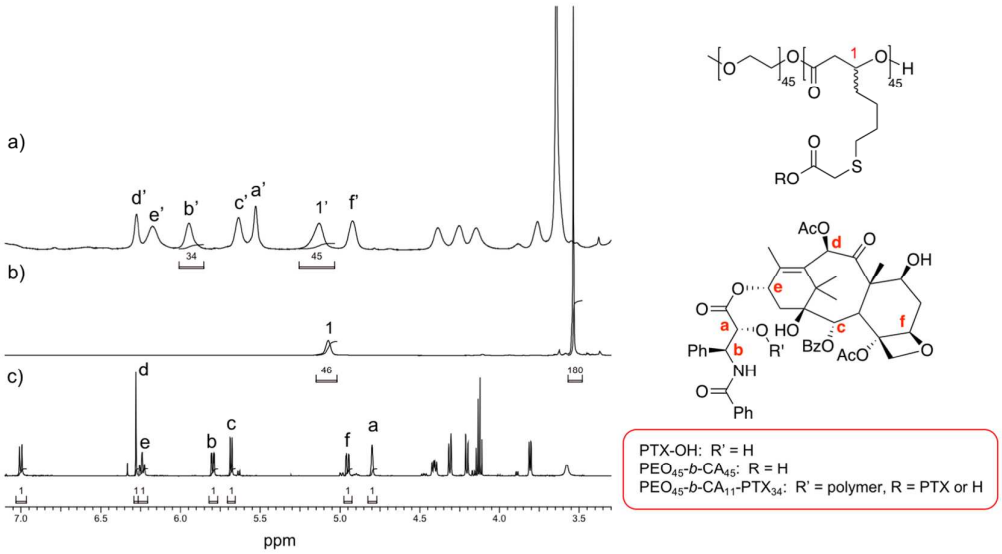

Fig 4. ^{1}H NMR spectra of a) PEO_{45}-*b*-CA_{11}-PTX_{34}, b) PEO_{45}-*b*-CA_{45}, and c) free paclitaxel (PTX-OH). The peaks labeled with ' indicate peaks corresponding to conjugated molecules.

indicated that 76% of the carboxylic acids on PEO_{45}-*b*-CA_{45} were esterified with PTX, resulting in ~34 PTX molecules per polymer. Further conversion of the carboxylic acids was not possible, likely due to the sterically bulky nature of the drug. SEC analysis provided an M_n of 9010 g mol^{-1} and a *Đ* of 1.88. While the M_w clearly increased as expected, the significant increase in *Đ* and underestimation of the M_n can likely be attributed to tailing due to interactions of the residual carboxylic acids with the column. DSC analysis showed that the copolymers were amorphous, with no melting transition observed for the PEO block. However, there was a large increase in the T_g to 131 °C due to the incorporation of PTX, which possesses a relatively rigid polycyclic structure and constitutes >70 wt% of the polymer.

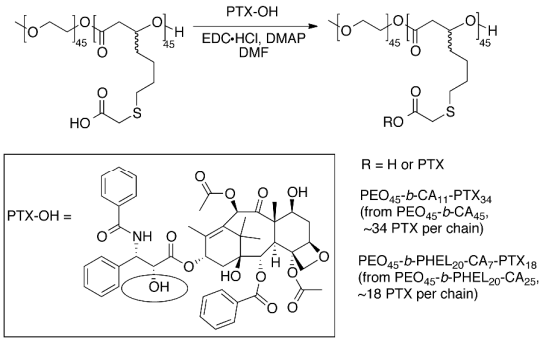

Scheme 3. Synthesis of the PTX conjugates PEO_{45}-*b*-CA_{11}-PTX_{34} and PEO_{45}-*b*-$PHEL_{20}$-CA_7-PTX_{18}. The site of conjugation on PTX is circled.

The self-assembly of PEO_{45}-*b*-CA_{11}-PTX_{34} was studied by the solvent exchange method involving THF and water. Unfortunately, macroscopic precipitation occurred under all of the conditions investigated, likely due to the very low *f* value of 0.05 for this polymer. Thus, PTX was also conjugated to PEO_{45}-*b*-$PHEL_{20}$-CA_{25} using the same procedure outlined above, affording PEO_{45}-*b*-$PHEL_{20}$-CA_7-PTX_{18}, with ~18 molecules of PTX

and ~7 residual carboxylic acids as indicated by ^{1}H NMR spectroscopy (Fig. S9). The *f* value calculated for this polymer was 0.08. This copolymer appears to self-assemble into small, solid spherical nanoparticles upon solvent exchange from THF to water, but these assemblies further aggregate to form micrometer-sized aggregates based on both DLS and TEM imaging (Figs. S42, S52). Thus, to obtain well-dispersed nanometer-sized assemblies, it would be necessary to further decrease the amount of PTX conjugated.

The labeling of polymer assemblies with fluorophores is also of significant interest for monitoring their cell uptake, intracellular trafficking, and biodistribution.[71-73] The covalent conjugation of the fluorophore ensures that the fluorophore does not diffuse out of the assembly and partition into hydrophobic environments such as cell membranes. In this work, the dye selected for conjugation was a rhodamine B derivative. To install a thiol onto the rhodamine for the thiol-ene reaction, 3-tritylsulfanylpropionic acid **1**[74] was first condensed using *N*, *N'*-dicyclohexylcarbodiimide (DCC) to form the anhydride **2** (Scheme 4). An amine-functionalized rhodamine **3**, was synthesized as previously reported,[75] then reacted with anhydride **2** to afford the protected thiol derivative **4**. Compound **4** was very sensitive to acid and required purification on neutral alumina rather than silica gel

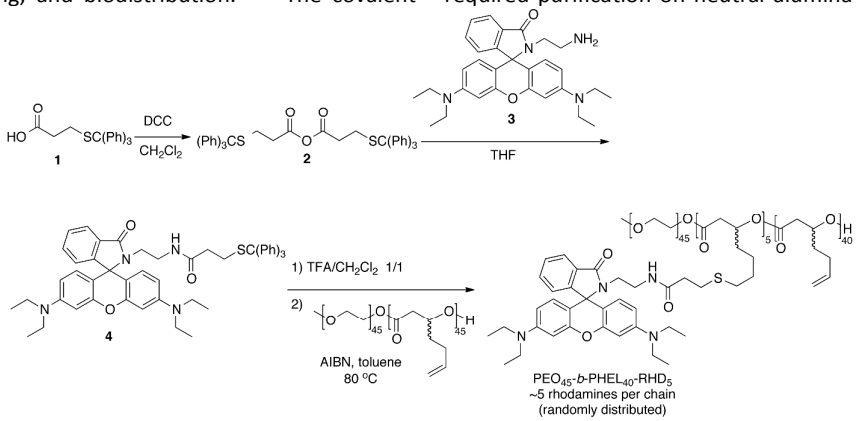

Scheme 4. Synthesis of a thiol-functionalized rhodamine derivative and its conjugation to PEO_{45}-*b*-$PHEL_{45}$ to afford PEO_{45}-*b*-$PHEL_{40}$-RHD_5

to avoid the loss of the trityl protecting group. The trityl group was then purposefully cleaved using trifluoroacetic acid (TFA) to afford the free thiol, which was used immediately in the conjugation reaction due to its susceptibility to oxidation and other degradation pathways.

First, conjugation of the dye to PEO_{45}-*b*-$PHEL_{45}$ was attempted using the photochemically-initiated thiol-ene reaction described above. This was unsuccessful, likely due to the strong absorbance of light by rhodamine. However, thermal initiation using azobisisobutyronitrile (AIBN) and 38 equiv. of thiol per polymer at 80 °C provided PEO_{45}-*b*-$PHEL_{40}$-RHD_5 with ~5 fluorophores per polymer as determined by ^{1}H NMR spectroscopy (Fig. S12). The reaction was not further optimized to achieve a higher conjugation yield. SEC provided an M_n of 6300 g/mol and a *Đ* of 1.15, which are very similar to those of PEO_{45}-*b*-$PHEL_{45}$. DSC analysis showed that PEO_{45}-*b*-$PHEL_{40}$-RHD_5 was amorphous, with no melting transition observed for the PEO block. There was also an increase in the T_g to -33 °C from -59 °C of PEO_{45}-*b*-$PHEL_{45}$. Self-assembly of PEO_{45}-*b*-$PHEL_{40}$-RHD_5 was investigated using the solvent exchange method. As shown in Fig. 3d and Table 4, this copolymer self-assembled to form solid spherical nanoparticles with a Z-average diameter of 102 nm. The larger size of these assemblies relative to those formed by PEO_{45}-*b*-$PHEL_{45}$ can likely be attributed to the decreased *f* of PEO_{45}-*b*-$PHEL_{40}$-RHD_5. The micelles were fluorescent with an emission λ_{max} of 456 nm (Fig. 5). This demonstrates that these new copolymers with pendant alkene groups can also be used to provide fluorescently-labeled polymer assemblies.

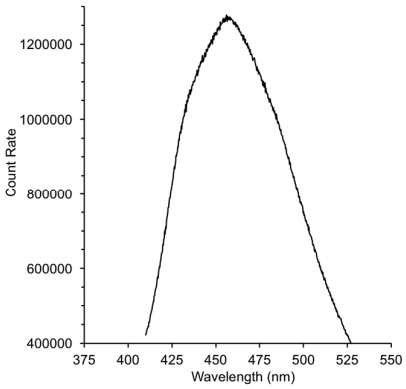

Fig. 5. Fluorescence emission spectrum of PEO_{45}-*b*-$PHEL_{40}$-RHD_5 micelles in water.

Conclusions

In this work, a small library of novel PEO-*b*-PHEL block copolymers with pendant allyl groups and varying PHEL lengths were synthesized. The parent polymers were studied for the formation of different morphologies and were found to produce solid spherical nanoparticles (PEO_{45}-*b*-$PHEL_{23}$ and PEO_{45}-*b*-$PHEL_{45}$) as well as vesicles (PEO_{45}-*b*-$PHEL_{79}$). The alkenes on the PHEL block of PEO_{45}-*b*-$PHEL_{45}$ were then

functionalized with octyl, TEG or carboxylic acid groups via UV-initiated thiol-ene chemistry, significantly changing the hydrophilic/hydrophobic balance of the copolymers and influencing their self-assembly behaviour to provide assemblies with different morphologies and stabilities. It was also demonstrated that the anti-cancer drug PTX could be conjugated to PEO_{45}-*b*-$PHEL_{20}CA_{25}$ via an ester linkage, although a further reduction in PTX content will be necessary in order to obtain well-dispersed aqueous assemblies. Finally, the conjugation of a rhodamine B thiol derivative by a thermally-initiated thiol-ene reaction was demonstrated, providing fluorescent assemblies. Thus, this work demonstrates that PEO-PHEL block copolymers serve as highly versatile backbones for the preparation of functional materials and assemblies for various applications.

Experimental section

Materials. PEO monomethyl ether (M_n = 2000) was purchased from Sigma Aldrich and was dried by three azeotropic distillations from toluene then stored in a nitrogen filled glovebox. β-6-HEL was synthesized by a procedure previously reported for similar lactones[54] and spectral data agreed with those previously reported.[76] The aluminum salen catalyst was synthesized according to a previously reported procedure.[77] 3-Tritylsulfanyl-propionic acid was prepared as previously described.[74] TEG-thiol was synthesized as previously reported.[78] Rhodamine derivative (**3**) was synthesized as previously reported.[79] EDC·HCl was purchased from Creo Salus (USA). Paclitaxel was purchased from Ontario Chemicals Inc. (Guelph, ON, Canada). CH_2Cl_2 was distilled from CaH_2 before use. Anhydrous THF, DMF and toluene were obtained from a solvent purification system using aluminum oxide columns. Deuterated solvents were purchased from Cambridge Isotopes Laboratories (Tewskbury, MA, USA). Solvents were purchased from Caledon Laboratory Chemicals (Georgetown, ON, Canada). All other chemical reagents were purchased from Sigma Aldrich (St. Louis, MO, USA) and were used as received.

General methods. Dialysis was performed using Spectra/Por 6 regenerated cellulose membranes with a molecular weight cut-off (MWCO) of either 3500 or 6000-8000 g mol^{-1} from Spectrum Laboratories (Rancho Dominguez, CA, USA). Nuclear Magnetic Resonance (NMR) spectroscopy was conducted on a Varian Inova 600 MHz Spectrometer (Varian, Palo Alto, CA, USA). All ^1H and ^{13}C NMR chemical shifts are reported in ppm and referenced relative to the residual solvent peaks ($CHCl_3$: ^1H δ = 7.26, ^{13}C δ = 77, DMSO-d_6: ^1H δ = 2.50, ^{13}C δ = 40). Coupling constants (*J*) are expressed in Hertz (Hz). Fourier transform infrared (FTIR) spectroscopy was conducted using a Bruker Tensor 27 spectrometer (Bruker, Billerica, MA, USA) in attenuated total reflectance mode (ATR) using a ZnSe crystal or a Perkin Elmer FTIR Spectrum Two Spectrometer (Waltham, MA, USA) in the universal attenuated total reflectance mode (UATR), using a diamond crystal as well as the UATR sampling accessory (part number L1050231). DSC was performed using a Q2000 from TA Instruments (New Castle, DE, USA) and TGA was performed on Q50 from TA Instruments. For TGA the heating rate was 10 ºC/min between 50-700 ºC under nitrogen. For DSC, the heating/cooling rate was 10 ºC min^{-1} from -100 to 150 ºC. Glass transition temperatures were obtained from the third or fourth heating cycle and were taken as the midpoint temperature of the transition. Size exclusion chromatography (SEC) was performed using a Visotek GPC Max VE2001 solvent module equipped with a Visotek VE3580 RI detector operating at 30 ˚C, an Agilent Polypore guard column (50 x 7.5 mm) and two Agilent Polypore (300 x 7.5 mm) columns connected in series. Samples were dissolved in THF (glass distilled grade) at a concentration of approximately 5 mg mL^{-1} and filtered (pore size: 0.22 μm, ProMax™ syringe filter, PTFE) then injected using a 100 uL loop. The THF eluent was filtered and eluted at 1 mL min^{-1} for a total of 30 minutes. Molar mass calibration was performed using polystyrene standards. The hydrodynamic radius of aggregates was measured by dynamic light scattering (Zetasizer Nano Series, Malvern Instruments, UK) at room temperature (25 ˚C) in a glass cuvette. The polymer concentration was ~ 1mg/mL. Transmission electron microscopy (TEM) images were acquired on a Phillips CM10 microscope operating at 80 kV with a 40 μm aperture. For TEM sample preparation, 5 μL of a ~0.2 mg mL^{-1} polymer assembly suspension was dropped directly on a TEM grid (Formvar/carbon film, 400 mesh, copper, Electron Microscopy Sciences, Hatfield, PA, USA) and allowed to evaporate to dryness over 16 hrs before image acquisition. No staining was performed. Fluorescence spectra were obtained using a QM-4 SE spectrometer from Photon Technology International (PTI) equipped with double excitation and emission monochromators.

Synthesis of PEO_{45}-*b*-$PHEL_{23}$ and general procedure for the synthesis of PEO-*b*-PHEL block copolymers. In a nitrogen filled glovebox, β-6-HEL (1.80 g, 14.3 mmol, 26 equiv), the aluminum salen catalyst [Al] (Scheme 1) (295 mg, 0.54 mmol, 1.0 equiv.) and monomethoxy-terminated PEO (M_n = 2000 g/mol, 1.08 g, 0.54 mmol, 1.0 equiv.) were added to an ampoule with toluene (20 mL). The ampoule was sealed, removed from the glovebox and placed in a preheated oil bath at 85 ˚C for 20 hours. After 20 hours, 0.5 mL of a 10% MeOH in CH_2Cl_2 solution was added to quench polymerization. A crude sample was taken for ^1H NMR spectroscopic analysis. The remainder was added to hexanes. Hexane was decanted and the remaining oil was dried until constant weight. Yield = 89%. ^1H NMR (600 MHz, $CDCl_3$): δ 1.70-1.71 (m, 49H), 2.02 – 2.11 (m, 51H), 2.50 – 2.61 (m, 49H), 3.38 (s, 3H), 3.64 (br s, 180H), 4.21 – 4.22 (m, 2H), 4.97 – 5.03 (m, 47H), 5.21 – 5.22 (m, 22H), 5.74 – 5.81 (m, 23H). M_n based on ^1H NMR spectroscopy = 4576 g mol^{-1}. SEC (THF): M_n = 5140 g mol^{-1}, M_w = 5550 g mol^{-1}, $Đ$ = 1.08. FTIR: 2891, 1737, 1642 cm^{-1}. T_m = 35 ˚C. T_g = -54 ˚C.

Synthesis of PEO_{45}-*b*-$PHEL_{21}$-$octyl_{24}$ and general procedure for functionalization of PEO_{45}-*b*-$PHEL_{45}$ block copolymers using UV-initiated thiol-ene chemistry. To a 10 mL Schlenk tube equipped with a stir bar, a solution of PEO_{45}-*b*-$PHEL_{45}$ (50.0 mg, 6.0 μmol), octanethiol (22.0 mg, 0.150 mmol) and DMPA (1.92 mg, 8.0 μmol) in toluene (1 mL) were added and the solution was degassed by bubbling through argon for 30 minutes. The reaction mixture was then placed in an ACE Glass

photochemistry cabinet containing a medium pressure mercury light source (450 W bulb, 2.8 mW cm^{-2} measured for UVA radiation at the sample position) and irradiated for 3 hours. The polymer was purified by precipitation into cold ethanol. Yield = 79%. ^{1}H NMR (600 MHz, $CDCl_3$): δ 0.88 (t, 72H, *J* = 7.0 Hz), 1.26 – 1.31 (m, 214H), 1.32-1.52 (m, 105H), 1.56-1.61 (m, 148H), 1.68-1.73 (m, 49H), 2.08 (m, 48H), 2.47 – 2.58 (m, 190H), 3.38 (s, 3H), 3.65 (br s, 180H), 4.22 (m, 2H), 4.97 – 5.04 (m, 41H), 5.20 (m, 44H), 5.75 – 5.81 (m, 20H). M_n based on ^{1}H NMR spectroscopy = 10549 g mol^{-1}. SEC (THF): M_n = 8150 g mol^{-1}, M_w = 9740 g mol^{-1}, $Đ$ = 1.19. FTIR: 2926, 2856, 1740, 1642 cm^{-1}. T_m = 34 ˚C. T_g = -60˚C.

Self-assembly of block copolymers by solvent exchange. The copolymer (8 mg) was dissolved in THF (1 mL) and stirred overnight and the resulting solution was filtered (pore size: 0.2 μm, DynaGard® syringe filter, PP). Polymer self-assembly was achieved by either the addition of polymer dissolved in THF (0.1 mL) to Milli Q-purified water (0.9 mL) while stirring rapidly or vice versa. Assemblies were stirred for 5 hours then the organic solvent was removed by dialysis using a 6000-8000 g mol^{-1} MWCO regenerated cellulose membrane in purified water overnight.

Procedure for self-assembly of PEO_{45}-*b*-$PHEL_{79}$ using a film hydration method. PEO_{45}-*b*-$PHEL_{79}$ (50 mg) was dissolved in 2 mL of CH_2Cl_2 in a 25 mL round bottom flask. A nile red solution in CH_2Cl_2 was then added to obtain 0.1 w/w/% of nile red relative to the copolymer. The CH_2Cl_2 was removed under a stream of nitrogen to produce a film of polymer on the flask. Deionized (DI) water (1 mL/10 mg of polymer) was added and the solution was stirred for 0.5 h at 55 °C. The solution was then sonicated for 0.5 h and finally stirred for 24 h at 55 °C. The resulting vesicles were characterized by confocal fluorescence microscopy using Zeiss LSM 510 DUO Vario using a 63x objective.

Acknowledgements

The authors thank the Natural Sciences and Engineering Research Council of Canada (Discovery Grant to ERG), the Ontario Graduate Scholarships program (BMR), the University of Edinburgh (JPM and MPS) and the Marie-Curie Actions Programme (Grant FP7-PEOPLE-2013-CIG-618372 to MPS) for funding this work.

Notes and references

1. Y. Mai and A. Eisenberg, *Chem. Soc. Rev.*, 2012, **41**, 5969-5985.
2. J. K. Kim, S. Y. Yang, Y. Lee and Y. Kim, *Prog. Polym. Sci.*, 2010, **35**, 1325-1349.
3. J. N. Albert and T. H. Epps, *Mater. Today*, 2010, **13**, 24-33.
4. C. T. Black, *ACS Nano*, 2007, **1**, 147-150.
5. M. Luo and T. H. Epps III, *Macromolecules*, 2013, **46**, 7567-7579.
6. D. J. Herr, *J. Mater. Res.*, 2011, **26**, 122-139.
7. K. Yan, H. Li, P. Li, H. Zhu, J. Shen, C. Yi, S. Wu, K. W. Yeung, Z. Xu, H. Xu and P. K. Chu, *Biomaterials*, 2014, **35**, 344-355.
8. J. Tang, Y. Sheng, H. Hu and Y. Shen, *Prog. Polym. Sci.*, 2013, **38**, 462-502.
9. A. Rösler, G. W. M. Vandermeulen and H.-A. Klok, *Adv. Drug Delivery Rev.*, 2012, **64**, 270-279.
10. Z. L. Tyrrell, Y. Shen and M. Radosz, *Prog. Polym. Sci.*, 2010, **35**, 1128-1143.
11. U. Prabhakar, H. Maeda, R. K. Jain, E. M. Sevick-Muraca, W. Zamboni, O. C. Farokhzad, S. T. Barry, A. Gabizon, P. Grodzinski and D. C. Blakey, *Cancer Res.*, 2013, **73**, 2412-2417.
12. H. Maeda, H. Nakamura and J. Fang, *Adv. Drug Delivery Rev.*, 2013, **65**, 71-79.
13. J. Nicolas, S. Mura, D. Brambilla, N. Mackiewicz and P. Couvreur, *Chem. Soc. Rev.*, 2013, **42**, 1147-1235.
14. H. M. Aliabadi, D. R. Brocks and A. Lavasanifar, *Biomaterials*, 2005, **26**, 7251-7259.
15. C. Allen, A. Eisenberg, J. Mrsic and D. Maysinger, *Drug Delivery*, 2000, **7**, 139-145.
16. S. Y. Kim, Y. M. Lee, H. J. Shin and J. S. Kang, *Biomaterials*, 2001, **22**, 2049-2056.
17. J. Ding, L. Chen, C. Xiao, L. Chen, X. Zhuang and X. Chen, *Chem. Commun.*, 2014, **50**, 11274-11290.
18. F. Ahmed, R. I. Pakunlu, G. Srinivas, A. Brannan, F. Bates, M. L. Klein, T. Minko and D. E. Discher, *Mol. Pharmaceutics*, 2006, **3**, 340-350.
19. S. Cai, K. Vijayan, D. Cheng, E. M. Lima and D. E. Discher, *Pharm. Res.*, 2007, **24**, 2099-2109.
20. K. Zhang, X. Tang, J. Zhang, W. Lu, X. Lin, Y. Zhang, B. Tian, H. Yang and H. He, *J. Controlled Release*, 2014, **183**, 77-86.
21. J. M. Anderson and M. S. Shive, *Adv. Drug Delivery Rev.*, 2012, **64**, 72-82.
22. M. A. Woodruff and D. W. Hutmacher, *Prog. Polym. Sci.*, 2010, **35**, 1217-1256.
23. K. S. Lee, H. C. Chung, S. A. Im, Y. H. Park, C. S. Kim, S.-B. Kim, S. Y. Rha, M. Y. Lee and J. Ro, *Cancer Res. Treat.*, 2008, **108**, 241-250.
24. J. Hrkach, D. Von Hoff, M. M. Ali, E. Andrianova, J. Auer, T. Campbell, D. De Witt, M. Figa, M. Figueiredo, A. Horhota and S. Low, *Sci. Transl. Med.*, 2012, **4**, 128ra139-128ra139.
25. N. Ajellal, C. M. Thomas and J.-F. Carpentier, *J. Polym. Sci. A: Polym. Chem.*, 2009, **47**, 3177-3189.
26. D. J. Stigers and G. N. Tew, *Biomacromolecules*, 2003, **4**, 193-195.
27. F. Sinclair, L. Chen, B. W. Greenland and M. P. Shaver, *Macromolecules*, 2016, **49**, 6826-6834.
28. N. J. Van Zee and G. W. Coates, *Chem. Commun.*, 2014, **50**, 6322-6325.
29. F. Jing and M. A. Hillmyer, *J. Am. Chem. Soc.*, 2008, **130**, 13826-13827.
30. G. L. Fiore, F. Jing, V. G. Young Jr., C. J. Cramer and M. A. Hillmyer, *Polym. Chem.*, 2010, **1**, 870-877.
31. R. Baumgartner, Z. Song, Y. Zhang and J. Cheng, *Polym. Chem.*, 2015, **6**, 3586-2590.
32. Y. Yan and D. J. Siegwart, *Polym. Chem.*, 2014, **5**, 1362-1371.
33. Q. Li, T. Wang, C. Ma, W. Bai and R. Bai, *ACS Macro Lett.*, 2014, **3**, 1161-1164.
34. J. Mandal, S. K. Prasad, D. S. Shankar Rao and S. Ramakrishnan, *J. Am. Chem. Soc.*, 2014, **136**, 2538-2545.
35. S. Ji, B. Bruchmann and H.-A. Klok, *Macromolecules*, 2011, **44**, 5218-5226.
36. C. Hoffmann, M. C. Stuparu, A. Daugaard and A. Khan, *J. Polym. Sci. Part A: Polym. Chem.*, 2015, **53**, 745-749.
37. C. Hahn, S. Wesselbaum, H. Keul and M. Möller, *Eur. Polym. J.*, 2013, **49**, 217-227.
38. S. Anantharaj and M. Jayakannan, *Biomacromolecules*, 2015, **16**, 1009-1020.
39. A. Kameyama, S. Watanabe, E.-I. Kobayashi and T. Nishikubo, *Macromolecules*, 1992, 2307-2311.

40. J. R. Lowe, M. T. Martello, W. B. Tolman and M. A. Hillmyer, *Polym. Chem.*, 2011, **2**, 702-708.
41. M. Constantin, C. I. Simionescu, A. Carpov, E. Samain and H. Driguez, *Macromol. Rapid Commun.*, 1999, **20**, 91-94.
42. C. Guillaume, N. Ajellal, J.-F. Carpentier and S. M. Guillaume, *J. Polym. Sci. A Polym. Chem.*, 2011, **49**, 907-917.
43. A. Mahmud, X. Xiong and A. Lavasanifar, *Macromolecules*, 2006, **39**, 9419-9428.
44. A. Mahmud, S. Patel, O. Molavi, P. Choi, J. Samuel and A. Lavasanifar, *Biomacromolecules*, 2009, **10**, 471-478.
45. A. Falamarzian and A. Lavasanifar, *Colloids Surf., B*, 2010, **81**, 313-320.
46. M. Shahin and A. Lavasanifar, *Int. J. Pharm.*, 2010, **389**, 213-222.
47. L. Timbart, E. Renard, M. Tessier and V. Langlois, *Biomacromolecules*, 2007, **8**, 1255-1265.
48. Y. Li, Y. Niu, D. Hu, Y. Song, J. He, X. Liu, X. Xia, Y. Lu and W. Xu, *Macromol. Chem. Phys.* , 2015, **216**, 77–84.
49. L. Yin, Y. Chen, Z. Zhang, Q. Yin, N. Zheng and J. Cheng, *Macromol. Rapid Commun.*, 2015, **36**, 483-489.
50. J. M. Harris, N. E. Martin and M. Modi, *Clin. Pharmacokinet.*, 2001, **40**, 539-551.
51. S. S. Banerjee, N. Aher, R. Patil and J. Khandare, *J. Drug Delivery*, 2012, **2012**, Article ID 103973.
52. A. B. Lowe, *Polym. Chem.*, 2010, **1**, 17-36.
53. C. E. Hoyle and C. N. Bowman, *Angew. Chem. Int. Ed.*, 2010, **49**, 1540-1573.
54. J. P. MacDonald, M. P. Parker, B. W. Greenland, D. Hermida-Merino, I. W. Hamley and M. P. Shaver, *Polym. Chem.*, 2015, **6**, 1445-1453.
55. J. T. Lee, P. J. Thomas and H. Alper, *J. Org. Chem.*, 2001, **66**, 5424-5426.
56. E. D. Cross, L. E. N. Allan, A. Decken and M. P. Shaver, *J. Polym. Sci., Part A: Polym. Chem.*, 2013, **51**, 1137-1146.
57. T. Wei, B. Zheng, H. Yi, Y. Gao and W. Guo, *Polym. Eng. Sci.*, 2014, **54**, 2872-2876.
58. R. Savic, L. Luo, A. Eisenberg and D. Maysinger, *Science*, 2003, **25**, 615-618.
59. D. E. Discher and F. Ahmed, *Annu. Rev. Biomed. Eng.*, 2006, DOI: 10.1146/, 323-341.
60. F. Ahmed and D. E. Discher, *J. Controlled Release*, 2004, **96**, 37-53.
61. D. E. Discher and A. Eisenberg, *Science*, 2002, **297**, 967-973.
62. E. R. Gillies and J. M. J. Fréchet, *Chem. Commun.*, 2003, 1640-1641.
63. F. Le Devedec, A. Won, J. Oake, L. Houdaihed, C. Bohne, C. M. Yip and C. Allen, *ACS Macro Lett.*, 2016, **5**, 128-133.
64. Y. Bae, N. Nishiyama, S. Fukushima, Y. Koyama, M. Yasuhiro and K. Kataoka, *Bioconjugate Chem.*, 2005, **16**, 122-130.
65. K. Ulbrich and V. Subr, *Adv. Drug Delivery Rev.*, 2010, **62**, 150.
66. X. Hu, J. Li, W. Lin, Y. Huang, X. Jing and Z. Xie, *RSC Adv.*, 2014, **4**, 38405.
67. A. Soleimani, M. M. A. R. Moustafa, A. Borecki and E. R. Gillies, *Can. J. Chem.*, 2014, **93**, 399-405.
68. R. Soleimani, A. Borecki and E. R. Gillies, *Polym. Chem.*, 2014, **5**, 7062-7071.
69. H. Lataste, V. Senilh, M. Wright, D. Guénard and P. Potier, *Proc. Natl. Acad. Sci. USA*, 1984, **81**, 4090-4094.
70. H. M. Deutsch, J. A. Glinski, M. Hernandez, R. D. Haugwitz, V. L. Narayanan, M. Suffness and L. H. Zalkow, *J. Med. Chem.*, 1989, **32**, 788-792.
71. M. P. Robin and R. K. O'Reilly, *Polym. Int.*, 2015, **64**, 174-182.
72. N. Rapoport, A. Marin, Y. Luo, G. D. Prestwich and M. Muniruzzaman, *J. Pharm. Sci.*, 2002, **91**, 157-170.
73. C. P. Lai, E. Y. Kim, C. E. Badr, R. Weissleder, T. R. Mempel, B. A. Tannous and X. O. Breakefield, *Nat. Commun.*, 2015, **6**, 7029.
74. K. S. Sharma, G. Durand, F. Giusti, B. Olivier, A. Fabiano, P. Bazzacco, T. Dahmane, C. Ebel, J. Popot and B. Pucci, *Langmuir*, 2008, **24**, 13581-13590.
75. X. Zhang, Y. Shiraishi and T. Hirai, *Org. Lett.*, 2007, **9**, 5039-5042.
76. J. T. Lee, P. J. Thomas and H. Alpher, *J. Org. Chem.*, 2001, **66**, 5424-5426.
77. D. A. Atwood, M. S. Hill, J. A. Jegier and D. Rutherford, *Organometallics*, 1997, **16**, 2659-2664.
78. A. W. Snow and E. E. Foos, *Synthesis*, 2003, **4**, 509-512.
79. J. Rull-Barrull, M. d'Halluin, E. Le Grognec and F.-X. Felpin, *Chem. Commun.*, 2016, **52**, 2525-2528.